Proc. of the 8th International Symposium on Geotechnical Safety and Risk (ISGSR)
Edited by Jinsong Huang, D.V. Griffiths, Shui-Hua Jiang, Anna Giacomini and Richard Kelly
 Published by Research Publishing, Singapore.
doi: 10.3850/978-981-18-5182-7_17-004-cd

Kriging-Based Conditional Random Field for Regional Liquefaction Potential Mapping Considering Statistical Uncertainty

Cong Miao[1], Zi-Jun Cao[2], Chang Tang[3] and Te Xiao[4]

[1]State Key Laboratory of Water Resources and Hydropower Engineering Science, Institute of Engineering Risk and Disaster Prevention, Wuhan University, 8 Donghu South Road, Wuhan 430072, P. R. China.
E-mail: miaocong@whu.edu.cn
[2]State Key Laboratory of Water Resources and Hydropower Engineering Science, Institute of Engineering Risk and Disaster Prevention, Wuhan University, 8 Donghu South Road, Wuhan 430072, P. R. China.
E-mail: zijuncao@whu.edu.cn (Corresponding Author)
[3]State Key Laboratory of Water Resources and Hydropower Engineering Science, Institute of Engineering Risk and Disaster Prevention, Wuhan University, 8 Donghu South Road, Wuhan 430072, P. R. China.
E-mail: tangchang@whu.edu.cn
[4]Department of Civil and Environmental Engineering, The Hong Kong University of Science and Technology, Hong Kong, China.
Email: xiaote@ust.hk

Abstract: Regional liquefaction potential assessment usually requires spatial interpolation based on probabilistic models (e.g., conditional random field, CRF). Accuracy of spatial interpolation relies highly on the number of testing data and stochastic model parameters. Since testing data is often insufficient,statistical uncertainty on model parameters is inevitable. Moreover, efficient CRF simulation across a large region is also of practical importance in engineering applications. In this paper, regional probabilistic characterization of the liquefaction severity index (LSI) calculated from cone penetration test (CPT)-based simplified procedure (SP) is presentedbased on Kriging-based CRF. With the proposed approach, the spatial variability and statistical uncertainty are, explicitly and simultaneously, considered through the ancestor sampling method (ASM) under a Bayesian framework. The proposed method is illustrated and validated using real CPT data. Results show that the proposed method provides reasonable spatial interpolation results of LSI values based on a limited number of CPT data, and the spatial variability and statistical uncertainty are taken into account in a quantifiable and rational way without compromising the computational efficiency of CRF simulation. Ignoring the statistical uncertainty might lead to underestimation of the prediction uncertainty.

Keywords: Bayesian;conditional random field;cone penetration test; liquefaction potential

1 Introduction

Earthquake-induced liquefaction of soils is one of the causes of the devastating damage (e.g., Kramer 1996; Ku et al. 2012). As a result, assessing the liquefaction potential of a liquefaction-prone area is critical. Among numerous methods, empirical simplified procedures (SP) based on in-situ tests, such as cone penetration test (CPT),are the most widely used methods for evaluating liquefaction potential (e.g., Seed and Idriss 1971;Zhang et al. 2002; Robertson 2009).However, SP only provides an estimate of liquefaction potential for a specific depth within an individual CPT sounding. An alternative approach using the liquefaction severity index (LSI) to quantify the liquefaction potential at testinglocationshas been developed over the past few decades (e.g., Iwasaki et al. 1982; Lee et al. 2004; Sonmez and Gokceoglu 2005). More importantly, understanding the spatial variability of LSI over a regionisoften of practical concern. Conditional random field (CRF), especially Gaussian CRF, is a useful technique to characterize the spatial variability in geological and geotechnical practice (e.g.,Li et al. 2016).

With a Gaussian CRF, the joint distribution among variables can be specified by the second-order statistics, namely mean valueμ and covariance matrix (or, equivalently, standard deviation (STD) σ and scale of fluctuation (SOF)λ given a correlation function). It is not possible to precisely obtain actual values of these statisticsbased on a limited number of measurements. In other words, estimates of CRF model parameters are inevitably associated with statistical uncertainty. Moreover, simulation of CRF for spatial variability characterization at a large-scale region is computationally expensive, particularlywhentesting locations are non-latticed (e.g., Xiao et al. 2018; Ching et al. 2020).

This paper develops a novel Bayesian framework integrating the empirical CPT-based SP with Kriging-based CRF simulation forefficiently probabilistic assessment of the regional liquefaction potential based on a limited number of CPT soundings at an area. Under the proposed framework, model parameters of CRF of LSI are inversely analyzed from LSI values calculated from CPT data at testing locations and their statistical uncertainties are quantified as well. This paper starts with descriptions of the empirical SP for evaluating LSI values at CPT locations. Then,CRF model parameters learning and CRF simulation are sequentially

implemented by the ancestor sampling method (ASM) under the proposed Bayesian framework. Finally, the proposed method is illustrated using real CPT data collected from Yuanlin, Taiwan.

2 CPT-based SP for EvaluatingLSIbased on CPT

LSI is a liquefaction potential indexconsidering both the severity of liquefaction and the depth of the liquefiable soil layers. It is evaluated using an integration of the calculated liquefaction probabilityP_L over depth together with a weighting function$W$,which is expressed as (e.g., Iwasaki et al. 1982; Sonmez and Gokceoglu 2005):

$$\mathrm{LSI} = \int_0^{20} P_L(z) W(z) dz \tag{1}$$

where $W(z) = 10 - 0.5z$ and z is the depth in meters.According to the literature (e.g., Ku et al. 2012), $P_L$can be calculated as:

$$P_L = 1 - \Phi\left(\frac{0.102 + \ln(F_S)}{0.276}\right) \approx \frac{1}{1 + (F_S / 0.9)^6} \tag{2}$$

where Φ is the standard normal cumulative distribution function; F_S is the factor of safety against the liquefaction at a given depth.In this study, aCPT-based empirical SP is employed to evaluate F_S,by which F_S is defined as the ratio between the cyclic resistance ratio (CRR) and cyclic stress ratio (CSR). Details of implementing the CPT-based SP for calculating F_S can be referred to Zhang et al. (2002) and Robertson (2009). Based on the CPT-based SP, LSI values at CPT locations can be obtained. However, CPTs are usually tested sparsely over a region in engineering practice.In the next section, Kriging-based CRF is used to assess the liquefaction potential at a region based on a limited number of CPTs.

3 Spatial Variability Characterization of LSI considering Statistical Uncertainty

Kriging-based CRF often assumes that the underlying random field is Gaussian (e.g., Bishop 2006). Considering that LSI defined in Eq. (1) has a lower bound at zero, it is assumed to follow the lognormal distribution. Correspondingly, the logarithm of LSI, denoted by ξ(i.e.,ln(LSI)), follows the Gaussian distribution. Herein, the CRF parameters include mean value μ, STD σ, and SOF λforξ. It is impossible to determine these parameters precisely based on the limited number, n, of CPT soundings, or$n$ LSI values calculated from CPT-based SP using the n CPT soundings.Let $\underline{\xi}^s = \left[\xi_1^s, \xi_2^s, \cdots, \xi_n^s\right]^T$, $\underline{\xi} = \left[\xi_1, \xi_2, \cdots, \xi_N\right]^T$, and $\underline{\theta} = \left[\mu, \sigma, \lambda\right]^T$, where $\underline{\xi}^s$ represent the logarithm ofLSI values at CPT locations and $\underline{\xi}$ is the logarithm of LSI values at the whole region of interest. From a probabilistic perspective, inferring $\underline{\xi}$ based on $\underline{\xi}^s$needs to specify possible values of CRF parameters$\underline{\theta}$ given $\underline{\xi}^s$. Using the Theorem of Total Probability, the conditional probability density function (PDF) $p\left(\underline{\xi}\middle|\underline{\xi}^s\right)$ is written as (e.g., Ang and Tang 2007):

$$p\left(\underline{\xi}\middle|\underline{\xi}^s\right) = \int p\left(\underline{\xi}, \underline{\theta}\middle|\underline{\xi}^s\right) d\underline{\theta} = \int p\left(\underline{\xi}\middle|\underline{\xi}^s, \underline{\theta}\right) p\left(\underline{\theta}\middle|\underline{\xi}^s\right) d\underline{\theta} \tag{3}$$

where $p\left(\underline{\theta}\middle|\underline{\xi}^s\right)$ is the conditional PDF of CRF parameters quantifying the statistical uncertainty of $\underline{\theta}$ given $\underline{\xi}^s$; $p\left(\underline{\xi}\middle|\underline{\xi}^s, \underline{\theta}\right)$ is the conditional PDF of $\underline{\xi}$ given$\underline{\theta}$and $\underline{\xi}^s$. As shown by Eq. (3), solving $p\left(\underline{\xi}\middle|\underline{\xi}^s\right)$ can be divided into two steps: characterizing the statistical uncertainty of the CRF model parameters based on $p\left(\underline{\theta}\middle|\underline{\xi}^s\right)$ and predicting LSI values at locations without CPTs using $p\left(\underline{\xi}\middle|\underline{\xi}^s, \underline{\theta}\right)$. These two steps are introduced in the following two subsections, respectively.

3.1 Characterizing Statistical Uncertainty of CRF Parameters

In this subsection, CRF model parameters$\underline{\theta}$are learned based on $\underline{\xi}^s$ within a Bayesian framework. Using Bayes' theorem, the posterior distribution $p\left(\underline{\theta}\middle|\underline{\xi}^s\right)$ of $\underline{\theta}$is given by (e.g., Wang et al. 2010):

$$p\left(\underline{\theta}\middle|\underline{\xi}^s\right) = Kp\left(\underline{\theta}\right) p\left(\underline{\xi}^s\middle|\underline{\theta}\right) \tag{4}$$

where K is a normalizing constant that is independent of $\underline{\theta}$, $p\left(\underline{\theta}\right)$ is the prior distribution of $\underline{\theta}$ for quantifying the knowledge on $\underline{\theta}$ in the absence of data; $p\left(\underline{\xi}^s\middle|\underline{\theta}\right)$ is the likelihood function reflecting the model fit between $\underline{\xi}^s$ and the random field model given $\underline{\theta}$.In the absence of prevailing information on $\underline{\theta}$, a joint uniform distribution is used and defined by relatively large ranges (i.e., $[\mu_{\min}, \mu_{\max}]$, $[\sigma_{\min}, \sigma_{\max}]$, and $[\lambda_{\min}, \lambda_{\max}]$) of μ, σ, and λ (e.g., Cao et al. 2016). As discussed in the preceding section, $\underline{\xi}^s$ is an n-by-1 Gaussian random vector with mean $\mu\underline{l}_n$and covariance $\mathbf{\Sigma}^s$ given $\underline{\theta}$.Then, $p\left(\underline{\xi}^s\middle|\underline{\theta}\right)$ is written as (e.g., Wang et al. 2010):

$$p\left(\underline{\xi}^s\middle|\underline{\theta}\right) \sim N\ \left(\mu\underline{l}_n, \mathbf{\Sigma}^s\right) \tag{5}$$

where$\underline{l}_n = [1, 1, \ldots, 1]^T$ is an n-by-1 vector; $\mathbf{\Sigma}^s = \sigma^2\mathbf{R}^s$; $\mathbf{R}^s$ is an n-by-n correlation coefficient matrix of $\underline{\xi}^s$, and can be calculated by a user-defined correlation function, such as the single exponential correlation function.In this study, an isotropic correlation function is adopted, and it has an identical λ value in different directions on the horizontal plane. Eq. (4) can be evaluated by various stochastic simulation methods. In this study, the Markov Chain Monte Carlo (MCMC) method, specifically the Metropolis-Hastings algorithm,is adopted to draw posterior samples of $\underline{\theta}$ from $p\left(\underline{\theta}\middle|\underline{\xi}^s\right)$(e.g., Cao et al., 2016).Subsequently, they can be used as inputs for predicting the logarithmic LSI values at locations without CPT soundings based on $p\left(\underline{\xi}\middle|\underline{\xi}^s, \underline{\theta}\right)$, as illustrated in the following subsection.

3.2 Predicting of LSI using Kriging-based CRF

From a Bayesian perspective, the conditional PDF $p\left(\underline{\xi}\middle|\underline{\xi}^s, \underline{\theta}\right)$ can also be defined as the posterior distribution of $\underline{\xi}$ given$\underline{\theta}$ and $\underline{\xi}^s$. As mentioned before, $\underline{\xi}$ and $\underline{\xi}^s$ are both assumed to be normally distributed given $\underline{\theta}$, i.e., $p\left(\underline{\xi}^s\middle|\underline{\theta}\right) \sim N\ \left(\mu\underline{l}_n, \mathbf{\Sigma}^s\right)$ and $p\left(\underline{\xi}\middle|\underline{\theta}\right) \sim N\ \left(\mu\underline{l}_N, \mathbf{\Sigma}\right)$, where $\mathbf{\Sigma}$ is an N-by-N covariance matrix among $\underline{\xi}$. Correspondingly, $p\left(\underline{\xi}\middle|\underline{\xi}^s, \underline{\theta}\right)$ is also a multivariate Gaussian posterior distribution, and it is written as (e.g., Bishop 2006):

$$p\left(\underline{\xi}\middle|\underline{\xi}^s, \underline{\theta}\right) \sim N\ \left(\mu\underline{l}_N + \left(\mathbf{\Sigma}^{sp}\right)^T \left(\mathbf{\Sigma}^s\right)^{-1} \left(\underline{\xi}^s - \mu\underline{l}_n\right), \mathbf{\Sigma} - \left(\mathbf{\Sigma}^{sp}\right)^T \left(\mathbf{\Sigma}^s\right)^{-1} \mathbf{\Sigma}^{sp}\right) \tag{6}$$

On the right-hand side of Eq. (6), the first term and the second term in parentheses are the posterior mean vector and covariance matrix of $\underline{\xi}$ given $\underline{\xi}^s$ and $\underline{\theta}$, respectively; $\mathbf{\Sigma}^{sp}$ is an n-by-N covariance matrix between $\underline{\xi}$ and $\underline{\xi}^s$.

On one hand, the dimension of $\underline{\xi}$ (i.e., N) might be extremely high for a large-scale region with a dense mesh defying the direct matrix decomposition method for CRF simulation. Although it can be partially tackled by Kronecker product providing that the correlation function is separable. However, it is compromised with the case that the CPT locations are non-latticed. Note that the dimension of $\underline{\xi}^s$ is usually smaller than that of $\underline{\xi}$, i.e., $n<<N$. It is relatively easy to calculate the mean term in Eq. (6), which is also known as the simple Krigingestimator (e.g., Journel 1974; Cressie 1993). Thus, kriging-based CRF is used in this study to, indirectly and numerically, simulate the spatial variability of $\underline{\xi}$ (i.e., $p\left(\underline{\xi}\middle|\underline{\xi}^s, \underline{\theta}\right)$) (e.g., Journel 1974). In the context of Kriging-based CRF, $\underline{\xi}$ is reconstructed as:

$$\underline{\xi} = \underline{\xi}^{sk} + \underline{\xi}^{urf} - \underline{\xi}^{urf,sk} \tag{7}$$

where $\underline{\xi}^{urf}$ is an unconditional random field (URF) realization of $\underline{\xi}$ over the whole region; $\underline{\xi}^{sk}$ and $\underline{\xi}^{urf,sk}$ are simple Krigingestimates based on $\underline{\xi}^{s}$ and $\underline{\xi}^{urf}$ realizations at CPT soundings, respectively. Because URF can be discretized into a regular mesh with equally spaced elements, URF realization can be simulated efficiently with the aid of Kronecker product, even though in a large region with a very fine mesh (e.g., Xiao et al. 2018).

To, explicitly and simultaneously, quantify the statistical uncertainty of $\underline{\theta}$ and the spatial variability of $\underline{\xi}$, the ancestor sampling method (ASM)(e.g., Bishop 2006) is adopted herein to sequentially generate the samples $\underline{\theta}$ and $\underline{\xi}$. Each set of posterior $\underline{\theta}$ samplesis used to simulate a set of $\underline{\xi}$ samples based on Eqs. (6) and (7). As a result, M realizations of $\underline{\theta}$ and $\underline{\xi}$ are obtained using ASM to numerically depict $p\left(\underline{\theta}\middle|\underline{\xi}^{s}\right)$ and $p\left(\underline{\xi}\middle|\underline{\xi}^{s}\right)$,respectively. The implementation of the proposed method with ASM is illustrated using real data in the following section.

4 Illustrative Example

For illustration, the proposed method is applied to evaluate the liquefaction potential of Yuanlin, Taiwan. The region concerned is 6.4km by 6km, as indicated by green lines in Figure 1. The liquefaction was widely manifested in this area causing significant damage to buildings, lifelines, and other facilities duringthe 1999 Chi-Chi earthquake. Following the earthquake, extensive field investigation in Yuanlin area was conducted, including in-situ and laboratory tests. Detailed ground conditions and geologic setting for this region can be referred to MAA (2000) and Juang et al. (2002).

Figure 1 shows Yuanlin map along with the layout of 40 CPT soundings by circles. Correspondingly, the LSI values calculated from CPT-based SP are also shown in Figure 1 by the size of circle.Input parameters of CPT-based SP consist of peak ground acceleration (PGA), earthquake magnitude (M_w), soil average unit weights above and under groundwater table (γ_a and γ_u), and atmosphere pressure (P_a), which are summarized in Table 1. The groundwater table is measured and recorded along with the CPT data. As shown in Figure 1, the calculated LSI values vary from approximately 0.0 to 65.0 in this region, and their logarithmic values are used as the input of the proposed method (i.e., $\underline{\xi}^{s}$) for liquefaction potential assessment.

Table 1. Input parameters of CPT-based SP for calculating LSI values (adopted from Juang et al. 2002)

Parameter	Value
PGA	0.19 g
M_W	7.25
γ_a	17.9 kN/m^3
γ_l	18.8 kN/m^3
P_a	101.325kPa

Figure 1. Yuanlin map showing the layout of CPT and the corresponding calculated LSI values

4.1 Characterizing Statistical Uncertainty of CRF Parameters

For Bayesian learning of CRFparameters, relatively large ranges (i.e., (0, 100], (0, 10], (0 km, 60 km]) forμ, σ, and λ are adopted to define the uniform prior distribution (e.g., Cao et al. 2016). Based on the diffuse prior distribution and 40 values of the logarithmic LSI, 10,000samples of $\underline{\theta}$ (i.e., M = 10,000) are drawn from Eq. (4) using the Metropolis-Hastings algorithm. Figure 2 shows the scatter plots and histograms of the 10,000 $\underline{\theta}$ samples, based on which the estimates including mean value, standard deviation, and coefficient of variation (COV)for each parameter arecalculated, as shown in Table 2. Because only a limited number of CPT soundings is available, the statistical uncertainty on $\underline{\theta}$ is considerably large, particularly for σ and λ,whose COVsbased on

posterior samples are relatively large (i.e., 0.29 and 0.48). Moreover, compared with μ and σ, the posterior marginal distribution of λ is more dispersed within the prior range (i.e., (0 km, 60 km]), implying that λ is more difficult to identify (e.g., Ching et al., 2016). Therefore, it is inappropriate to ignore the statistical uncertainty of $\underline{\theta}$ for CRF simulation. It is reasonable to incorporate the statistical uncertainty on $\underline{\theta}$ into thespatial variabilitycharacterization through CRF.

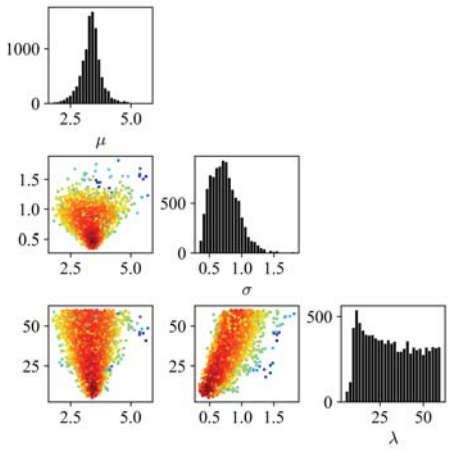

Figure 2. Posterior samples and marginal distributions of CRF parameters in Yuanlin area

Table 2. Statistics of posterior samples for CRF parameters

	μ	σ	λ
Mean value	3.35	0.74	32.0 km
Standard deviation	0.43	0.21	15.3 km
Coefficient of variation	0.13	0.29	0.48

4.2 Mapping LSI in Yuanlin Region

Based on the $\underline{\theta}$ samples obtained in the preceding subsection, the corresponding 10,000samples of $\underline{\xi}$ are simulated using Eqs. (6) and (7), for which the region is discretized as 201 by 201 square elements. As a result, 10,000 realizations of $\underline{\xi}$ can be efficientlysimulated from the proposed method.In implementation, the large covariance matrix with the size of 40,401 by 40,401 can be decomposed as two small matrixes with the dimension of 201 by 201.Then, they are transformed into the LSI field by taking the exponential. Each simulation represents one realization of LSI values given a $\underline{\theta}$ sample, which quantifies the spatial variability of LSI across a region. According to 10,000 $\underline{\xi}$ samples, statistics (including mean value and STD) can be calculated for facilitating regional liquefaction potential assessment.

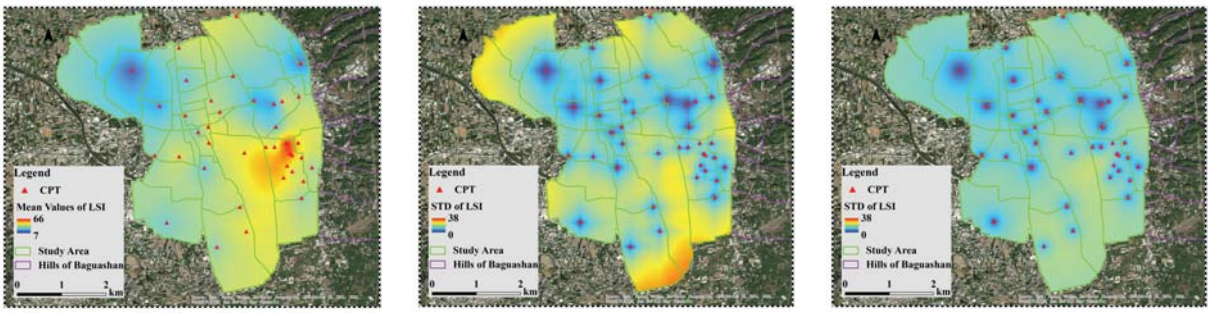

(a) mean values (b) STDs (c) STDs based on MPVs of $\underline{\theta}$

Figure 3. Results of CRF simulations for LSI using the proposed method in Yuanlin area

Figure 3(a) and 3(b) show the mean value and STD of LSI over the region by the color scale, in which the CPT locations are also plotted for reference. Forcomparison,Figure 3(c) plots the STD of LSI based on the most probable values (MPVs) of $\underline{\theta}$, i.e., $\mu = 3.40$, $\sigma = 0.45$, and $\lambda = 9.98$ km.The spatial pattern of the predicted mean value of LSI shown in Figure 3(a) is generally consistent with the calculated LSI values shown in Figure 1. This indicates that the proposed method can make proper use of the site information.As shown in Figure 3(b), it is observed that the STD around testing locations is relatively small and reaches to zero at CPT locations. This indicates that the proposed method depends highly on the calculated LSI values and the predicted LSI values around CPT locations are more reliable.In addition, considering that the statistical uncertainty of $\underline{\theta}$ has been incorporated into the spatial variability characterization, the STD of LSI away from CPT locations is relatively large (see Figure 3 (b) and (c)). Without considering the statistical uncertainty, the prediction uncertainty might be underestimated.

5 Summary and Conclusion

This paper presents a Bayesian framework for probabilistic characterization of the regional liquefaction potential based on a limited number of cone penetration test (CPT) data in a liquefaction-prone region. Within the proposed framework, the statistical uncertainty and spatial variability are, explicitly and quantitatively, considered for regional mapping the liquefaction severity index (LSI). To tackle the computational issue for conditional random field (CRF) simulation at a large region, simple Kriging-based CRF is adopted herein, with which Kronecker product can be used for efficient CRF simulation without the need of latticed locations of CPT soundings. The proposed method is implemented using the ancestor sampling method (ASM), and it was illustrated using real CPT data at Yuanlin, Taiwan. Results showed that the proposed approach deals, rationally, with the statistical uncertainty and spatial variability for characterizing LSI. Based on a limited number of CPT soundings, the statistical uncertainty on CRF model parameters is inevitable. Thus, the prediction uncertainty on LSI might be underestimated only using a single set $\underline{\theta}$, which ignores the statistical uncertainty of CRF parameters in simulation.

Acknowledgment

This work was supported by the NationalNatural Science Foundation of China (Project Nos. 51879205,51779189). The financial support isgratefully acknowledged.

References

Ang, A. H., Tang, W. H. (2007). Probability concepts in engineering planning: emphasis on applications to civil and environmental engineering. *John Wiley and Sons*

Bishop, C. M. (2006). Pattern recognition and machine learning.*New York: Springer*

Cao, Z. J., Wang, Y., Li, D. Q. (2016). Site-specific characterization of soil properties using multiple measurements from different test procedures at different locations - A Bayesian sequential updating approach. *Engineering Geology*, 211: 150-161.

Ching, J. Y., Phoon, K. K., Wu, S. H. (2016). Impact of statistical uncertainty on geotechnical reliability estimation. *Journal of Engineering Mechanics*, 142(6): 04016027.

Ching, J. Y., Huang, W. H., Phoon, K. K. (2020). 3D probabilistic site characterization by sparse Bayesian learning. *Journal of Engineering Mechanics*, 146(12): 04020134.

Cressie, N. (1993). Statistics for spatial data. *John Wiley & Sons.*

Iwasaki, T., Tokida, K. I., Tatsuoka, F., Watanabe, S., Yasuda, S., & Sato, H. (1982). Microzonation for soil liquefaction potential using simplified methods. *In Proceedings of the 3rd international conference on microzonation, Seattle* (Vol. 3, No. 2, pp. 1310-1330).

Journel, A. G. (1974). Geostatistics for conditional simulation of ore bodies. *Economic Geology*, 69(5): 673-687.

Juang, C. H., Yuan, H., Lee, D. H., & Ku, C. S. (2002). Assessing CPT-based methods for liquefaction evaluation with emphasis on the cases from the Chi-Chi, Taiwan, earthquake. *Soil Dynamics and Earthquake Engineering*, 22(3), 241-258.

Kramer, S. L. (1996). Geotechnical earthquake engineering.*Pearson Education India.*

Ku, C. S., Juang, C. H., Chang, C. W., & Ching, J. (2012). Probabilistic version of the Robertson and Wride method for liquefaction evaluation: development and application. *Canadian Geotechnical Journal*, 49(1), 27-44.

Lee, D. H., Ku, C. S., & Yuan, H. (2004). A study of the liquefaction risk potential at Yuanlin, Taiwan. *Engineering Geology*, 71(1-2), 97-117.

Li, X. Y., Zhang, L. M., Li, J. H. (2016). Using conditioned random field to characterize the variability of geologic profiles. *Journal of Geotechnical and Geoenvironmental Engineering*, 142(4): 04015096.

MAA (2000). Soil Liquefaction Assessment and Remediation Study, Phase I (Yuanlin, Dachun, and Shetou), Summary Report and Appendixes, *Moh and Associates (MAA), Inc., Taipei, Taiwan (in Chinese)*.

Robertson, P. K. (2009). Performance based earthquake design using the CPT. *Proc. IS-Tokyo*, 3-20.

Seed, H. B., and Idriss, I. M. (1971). Simplified procedure for evaluatingsoil liquefaction potential. *Journal of Geotechnical and Geoenvironmental Engineering*, 97(9), 1249–1273.

Sonmez, H., & Gokceoglu, C. (2005). A liquefaction severity index suggested for engineering practice. *Environmental Geology*, 48(1), 81-91.

Wang, Y., Au, S. K., Cao, Z. J. (2010). Bayesian approach for probabilistic characterization of sand friction angles. *Engineering Geology*, 114(3-4): 354-363.

Xiao, T., Li, D. Q., Cao, Z. J., Zhang, L. M. (2018). CPT-based probabilistic characterization of three-dimensional spatial variability using MLE. *Journal of Geotechnical and Geoenvironmental Engineering*, 144(5): 04018023.

Youd, T. L., Idriss, I. M. (2001). Liquefaction resistance of soils: Summary report from the 1996 NCEER and 1998 NCEER/NSF workshops on evaluation of liquefaction resistance of soils. *Journal of Geotechnical and Geoenvironmental Engineering*, 127(4): 297-313.

Zhang, G., Robertson, P. K., & Brachman, R. W. (2002). Estimating liquefaction-induced ground settlements from CPT for level ground. *Canadian Geotechnical Journal*, 39(5), 1168-1180.